JOURNAL OF MATERIALS SCIENCE 21 (1986) 1502–1508

Properties of composites of 2014 aluminium alloy with Ni–Mo-based metallic glass particles

A. K. JHA*, G. S. UPADHYAYA‡, P. K. ROHATGI*
*Regional Research Laboratory (Bhopal), Council of Scientific & Industrial Research, Near Habibganj Naka, Hoshangabad Road, Bhopal 462 026, Madhya Pradesh, India
‡Department of Metallurgical Engineering, Indian Institute of Technology Kanpur, IIT Kanpur PO, Kanpur 208 016, Uttar Pradesh, India

Composites of 2014 aluminium alloy containing dispersions of metallic glass particles (51.5 wt% Ni, 38.0 wt% Mo, 8.0 wt% Cr and 1.5 wt% B) have been prepared by a conventional powder metallurgy route involving powder mixing, compaction, sintering and heat treatment. Physical and mechanical properties of the composites, such as dimensional changes, hardness, electrical resistivity and corrosion behaviour, were studied. Dimensional growth up to a maximum of 6% in a linear direction was observed in all sintered composites. Hardness *Hv* increased from 40 to 55 kg mm^{-2} with the addition of 4 vol% of dispersoid, followed by a gradual decrease with increasing additions of dispersoid. The decrease in hardness above 4 vol% of dispersoid was attributed to the presence of increasing amounts of porosity. Electrical resistivity increased from 50 nΩ m (for 2014 aluminium alloy) to 180 nΩ m at 20 vol% dispersoid. The corrosion rate in an artificial sea water environment decreased linearly with the volume fraction of dispersoid. Re-pressing and re-sintering (in an argon atmosphere) of composites containing 4 vol% of metallic glass particles resulted in an increase in *Hv* from 55 (argon sintering) to 83 kg mm^{-2}, and a decrease in electrical resistivity from 57 to 52 nΩ m due to the increase in density. The corrosion rate in an artificial sea water environment of composites containing 4 vol% of metallic glass decreased from 70×10^{-3} to 50×10^{-3} mg dm^{-2} per day due to re-pressing and re-sintering.

1. Introduction

Aluminium, in addition to its inherent properties, can attain a wide range of properties by the addition of alloying elements, the incorporation of dispersoids and by thermomechanical processing. The variation in properties of powder-metallurgy (P/M) produced aluminium alloy compacts have been discussed by a number of authors [1–4] as a function of compaction pressure, sintering time, temperature and atmospheres. The effects of ceramic dispersoids on the properties of aluminium alloys have also been reported [5–8].

Recently, some work has been reported on the effect of the addition of second-phase particles on the age-hardening characteristics of aluminium alloys [9, 10]. It was observed [9] that, in the presence of more than 1.5 vol % of Al_2O_3, Guinier–Preston (GP) zone formation was completely inhibited during natural ageing and the advantage of artificial ageing was also lost. However, Wilcox [10] has reported that addition of 12 vol % Al_2O_3 resulted in higher recrystallization temperature and creep strength at elevated temperatures in 7075 and 2024 aluminium alloys. The effects of dispersoids of varying hardness on the properties of sintered 2014 aluminium alloy have been reported by the present authors [11, 12].

In this paper studies on composites of 2014 aluminium alloy as matrix, and metallic glass particles (Ni–Mo-based) as dispersoids, have been carried out. The preparation and properties of such composites are reported here.

2. Experimental details

Aluminium premix 2014 powder (MD 24 grade) obtained from Alcan Ingot and Powders, Elizabeth, New Jersey, and MarkoMet 1064 metallic glass powder obtained from Marko Materials Inc., Billerica, Massachusetts, were used in the present study. Table I lists the powder characteristics of the raw materials used in the present investigation.

The aluminium alloy (powder premix) was blended with 4, 8, 12, 16, and 20 vol % of the dispersoid (metallic glass) thoroughly for 2 h, in a double cone blender (Model 529 from Netzsch, Selb/Bayern, West Germany). Green cylindrical pellets of 12.7 mm diameter and ~15 mm height were compacted at a pressure of 310 MPa on a single-acting hydraulic press. Green compacts were sintered in argon (dew point < −35° C), vacuum (1.33×10^{-7} MPa pressure) and nitrogen (dew point > −20° C) at temperatures of 550 and 570° C for 0.5 h. A proportional temperature controller was used to give temperature control to

0022–2461/86 $03.00 + .12

TABLE I Powder characteristics of 2014 aluminium alloy premix and metallic glass

Material	Composition (wt %)
Aluminium premix (2014)	
Aluminium	93.8
Copper	4.4
Magnesium	0.5
Silicon	0.9
Manganese	0.4
Lubricant	1.5
Flow rate: not free flowing	
Apparent density: 1.28 mg m^{-3}	
Particle size (mesh)	
+200	43
+250	11
+325	12
+400	5
−400	21
MarkoMet 1064	
Nickel	51.5
Molybdenum	38.0
Chromium	8.0
Boron	1.5
Flow rate: 20 sec per 50 g	
Apparent density: 4.5 mg m^{-3}	
Particle size: −250 to 325 (all)	

within ±1° C. Sintered composites were solution-treated at 510° C for 0.5 h, quenched in water and aged at 175° C for 8 h. One set of composites, sintered at 570° C, was re-pressed under a pressure of 780 MPa in a tungsten carbide lined die, and re-sintered at 510° C in the respective atmosphere for 0.5 h followed by quenching and ageing as mentioned earlier.

The physical dimensions and weights of green and sintered compacts were measured. Densities and porosities were obtained by a method described by Arthur [13]. The densification parameter was calculated from the following formula:

$$\Delta D = \frac{(\text{sintered density}) - (\text{green density})}{(\text{theoretical density}) - (\text{green density})}$$

Vickers hardness was measured using a load of 25 N. Optical metallography of selected specimens was also carried out. The electrical resistivity of age-hardened samples was measured on a conductivity meter Type 757 (Technofour, Pune, India), which works on an eddy-current principle. The corrosion behaviour of composites sintered at 570° C in argon, aged and re-pressed, and re-aged was studied using an artificial sea water medium at room temperature for 70 days. Plots of corrosion loss in mg dm^{-2} per day (MDD) against the volume fraction of dispersoid were recorded.

3. Results

3.1. Effect of sintering atmosphere and temperature

Fig. 1 shows the changes in the dimensions of composites with respect to the volume fraction of the dispersoid. The dimensions increased with an increase in the amount of dispersoid in all cases. Compacts swelled more after sintering at 570° C than after sintering at 550° C. Maximum swelling was observed in composites after vacuum sintering. In many cases the plots reveal the presence of maxima at some specific dispersoid fraction. The sintered density of composites increased with increasing amount of dispersoid irrespective of the sintering atmosphere (Fig. 1). At the sintering temperature of 550° C, dispersoid additions up to 20 vol % had hardly any influence on densification except in the case of vacuum sintering. At elevated sintering temperature (570° C), the growth of compacts decreased with increase in dispersoid content, in the order vacuum → nitrogen → argon (Fig. 1).

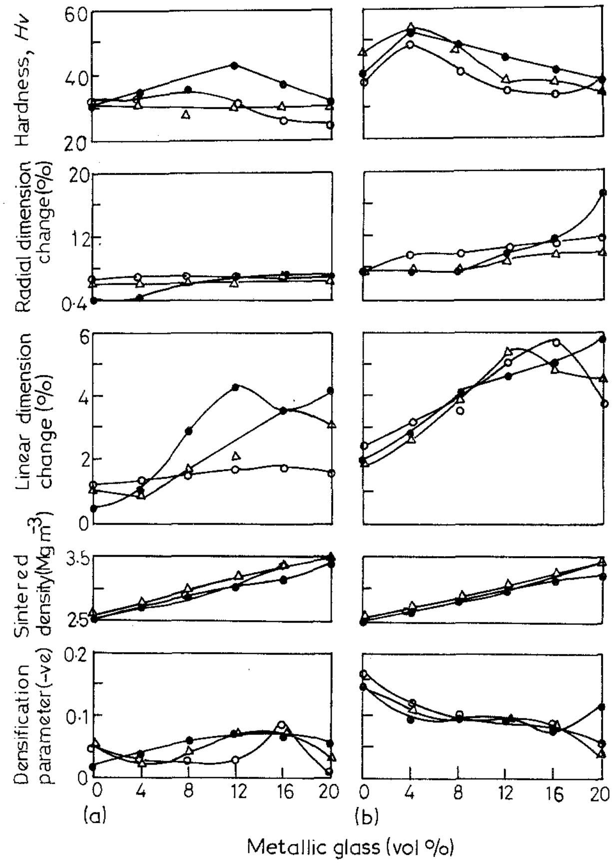

Figure 1 Properties of 2014 aluminium alloy based composites as a function of volume percentage of metallic glass particles, sintering atmosphere (argon, vacuum or nitrogen) and sintering temperature: (a) 550° C, (b) 570° C; (●) vacuum, (○) nitrogen, (△) argon.

Fig. 1 also shows the hardness of compacts in the as-sintered condition. Sintering at 570° C resulted in greater hardening as compared to sintering at 550° C in almost all cases. The hardness of all compacts sintered at 550° C remained more or less the same irrespective of the amount of dispersoid, with the exception of the composite containing 12 vol % of dispersoid sintered in a vacuum. Composites having 4 vol % of dispersoid attained peak hardness in the as-sintered condition. Sintering in an argon atmosphere resulted in maximum hardness.

Optical micrographs of the aluminium alloy and its composites are shown in Fig. 2. It can be seen that there is a considerable amount of porosity in both the base alloy and the composites. While the dispersoids show an even distribution, they are quite frequently surrounded by interfacial porosities in composites.

3.2. Effect of re-pressing and age-hardening

Figs. 3 to 5 show the hardness variation in composites

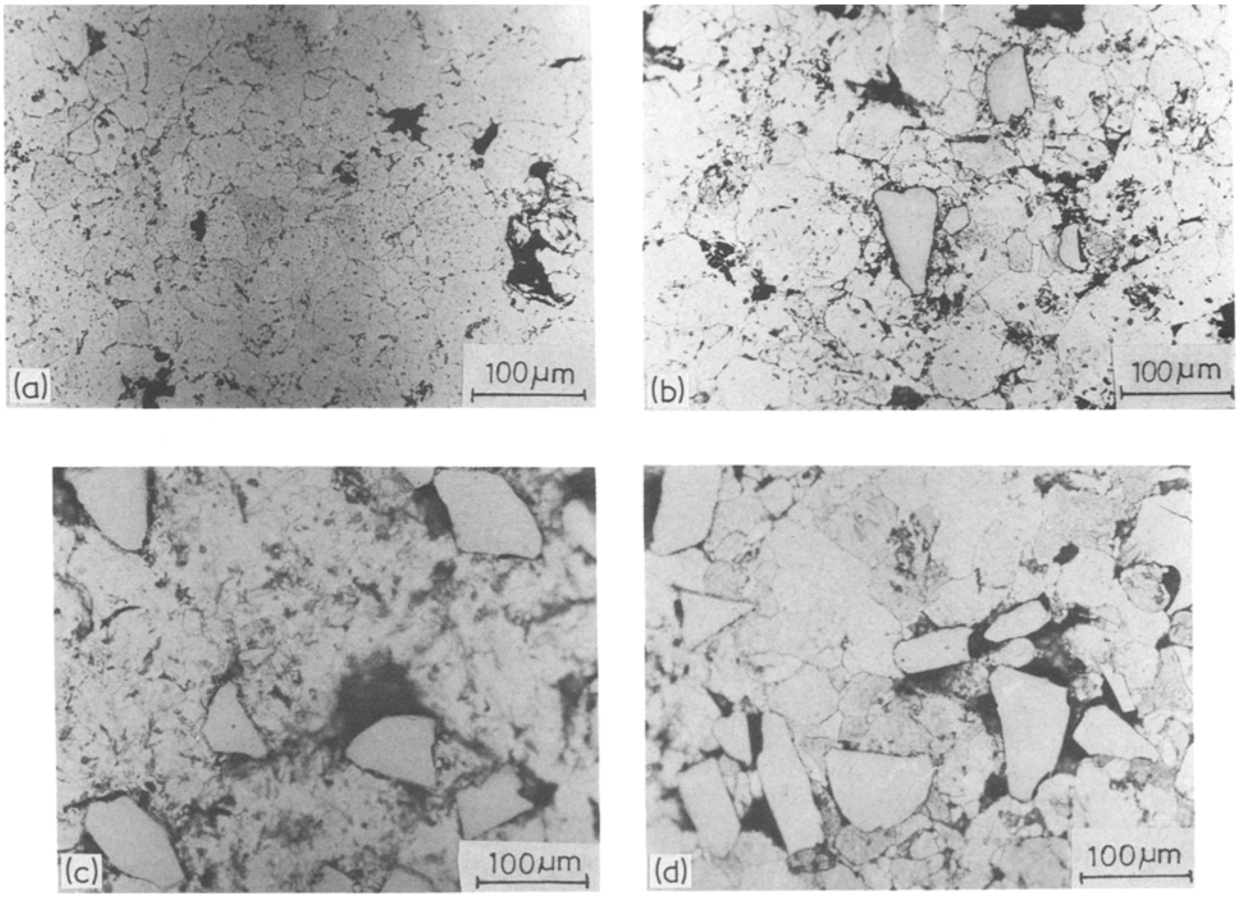

Figure 2 Optical micrographs of (a) 2014 aluminium alloy, and 2014 alloy containing (b) 4 vol % (c) 12 vol % and (d) 20 vol % of metal glass particles, sintered at 570° C in an argon atmosphere.

after re-pressing, re-sintering and ageing treatments. Corresponding densities and porosities of sintered, re-pressed and quenched composites have been incorporated in the plots. Re-pressing–re-sintering improved the densificiation. For example, the porosity of the composite containing 20 vol % dispersoid decreased from 39 to 33% (Fig. 3) due to re-pressing and re-sintering.

Age-hardening after sintering considerably improved the hardness values of the composites, the peak hardness still being obtained at 4 vol % of dispersoid. After re-pressing, the hardness of the composite increased considerably; the maximum increase is of the order of 50% (in the case of argon-sintered composites). Age-hardening treatment of re-pressed compacts was effective, but not to the extent observed for the as-sintered compacts.

Plots of electrical resistivity show that it increased with increase in volume fraction of the dispersoid. After re-pressing, the resistivity of the compacts decreased in almost all cases.

Fig. 6 shows the effect of dispersoid on the

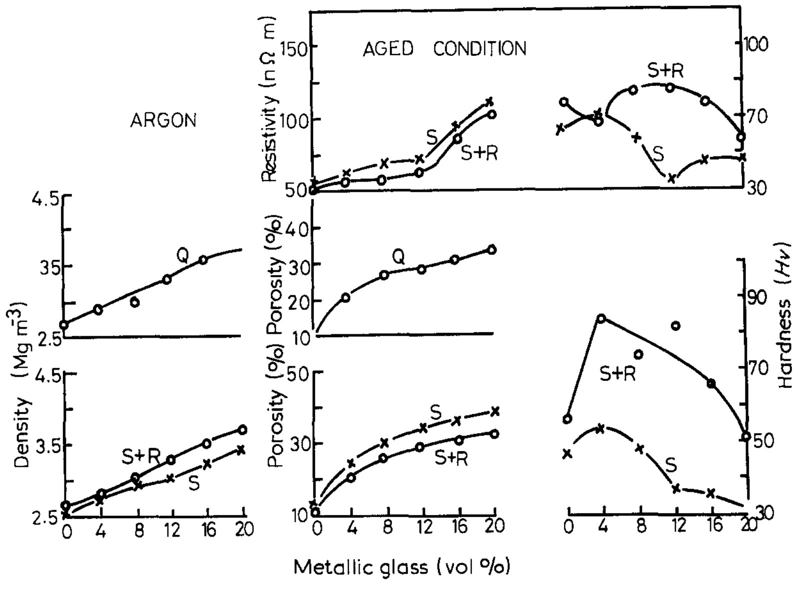

Figure 3 Effect of re-pressing and age-hardening on the properties of 2014 aluminium based composites sintered in an argon atmosphere. S = sintered, R = re-pressed, Q = quenched.

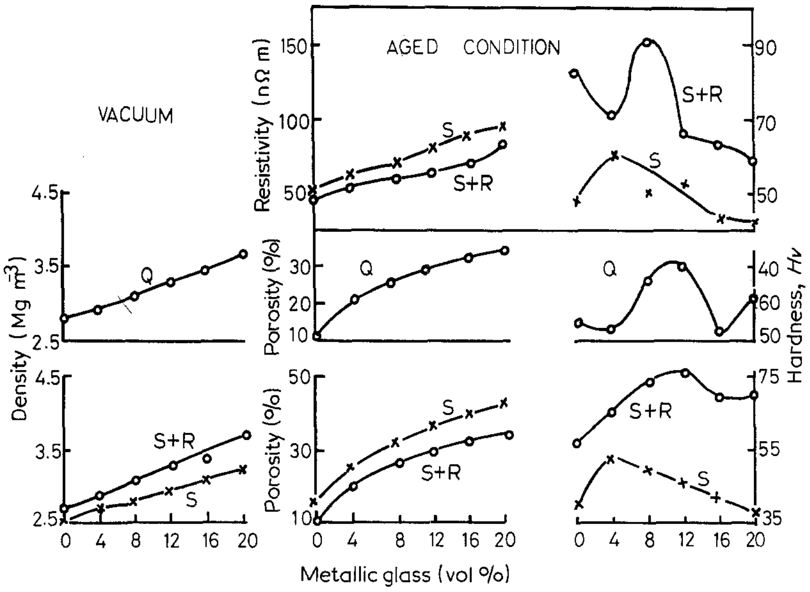

Figure 4 Effect of re-pressing and age-hardening on the properties of 2014 aluminium alloy based composites sintered in a vacuum. S = sintered, R = re-pressed, Q = quenched.

corrosion rate of composites held in artificial sea water for 70 days at room temperature. It shows that the corrosion rate decreased with increasing amount of dispersoid. It is also evident from Fig. 6 that re-pressed and re-aged samples showed a lesser corrosion rate than as-sintered and aged ones.

4. Discussion

4.1. Dimensional behaviour

Dimensional growth of compacts of either 2014 base aluminium alloy or composites occurred after sintering at both temperatures, i.e. 500 and 570° C, the higher temperature giving more dimensional growth. Similar observations have been explained in the literature on the basis of an enhanced volume fraction of liquid phase aiding sintering [14]. The eutectic temperature of Al–Cu binary is 548° C [15] and hence it is probable that at 550° C adequate eutectic liquid may not have formed to activate densification. In order to test this hypothesis, electron probe microanalysis (EPMA) traces were taken on metallographic sections of composites containing 4 vol % of dispersoid sintered at 570° C (Fig. 7a) and 550° C (Fig. 7b). The region shown between the arrows in Figs. 7a and b indicates the dispersoid particles shown in the corresponding micrographs of Fig. 8a and b. It can be seen from the copper trace in Fig. 7b that copper is not uniformly distributed in the matrix of the sample sintered at 550° C, whereas the EPMA traces of the sample sintered at 570° C (Fig. 7a) shows a uniform distribution of copper over the entire region of the scan. It has been reported [16] that sintering at a temperature lower than 560° C produces a small amount of eutectic liquid from a fraction of aluminium and copper particles, the rest of the copper particles remaining in an elemental form in premixed Al–Cu compacts. Uneven copper peaks in Fig. 7b suggest the possible presence of copper particles in elemental form. In contrast, the uniform distribution of copper in composites after sintering at 570° C suggests adequate liquid-phase sintering. Secondly, enhanced swelling at higher sintering temperature could be due to the presence of closed porosity which is likely to exert a hydrostatic pressure under the influence of temperature. It should also be noted from Fig. 1 that at the lower sintering temperature (550° C), the densification parameter was practically unaffected by the addition of dispersoid.

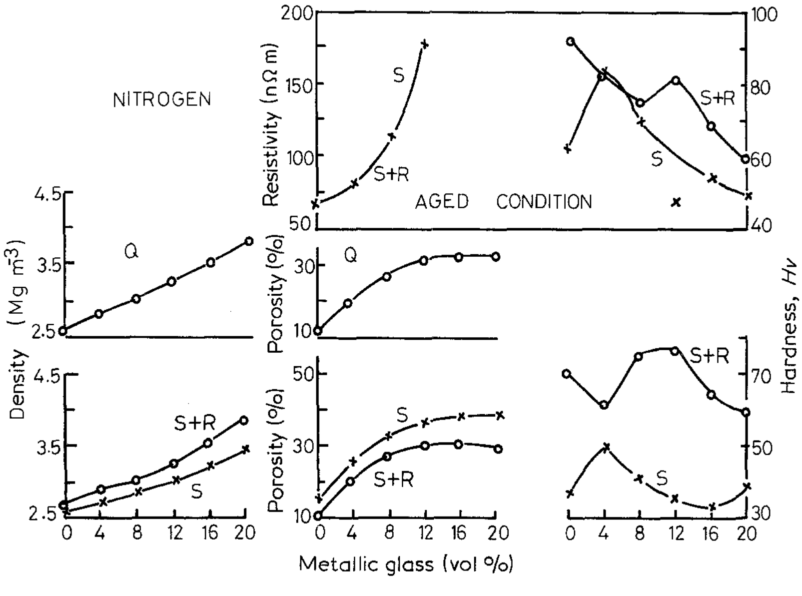

Figure 5 Effect of re-pressing and age-hardening on 2014 aluminium alloy based composites sintered in a nitrogen atmosphere. S = sintered, R = re-pressed, Q = quenched.

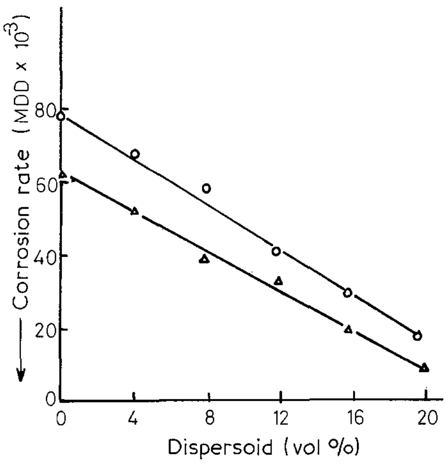

Figure 6 Variation with volume fraction of metallic glass particles of corrosion rate of 2014 aluminium alloy and its composites sintered at 570° C, re-pressed and re-sintered. MDD = mg dm^{-2} per day. (○) sintered, (△) re-pressed and re-sintered.

4.2. Hardness

It has been observed that the hardness of composites sintered at 570° C is higher than that of composites containing the same volume of dispersoid sintered at 550° C (Fig. 1). This again could be attributed to liquid-phase sintering occurring at 570° C. A hardness increase in *Hv* from 40 to 50 kg mm^{-2} with the addition of 4 vol % dispersoid was followed by a gradual decrease. The reduction in the hardness beyond 4 vol % of dispersoid could be attributed to the higher amount of porosity (> 20%), when the amount of dispersoid exceeded 4 vol % of dispersoid. It is also evident from EPMA data (Figs. 7 and 8) that there is practically no interaction between the matrix and the dispersoid. Optical micrography (Fig. 2) clearly shows localized porosity around the particles. This is why the addition of very hard particles (metallic glass with *Hv* = 900) to the relatively soft matrix did not result in the corresponding increase in

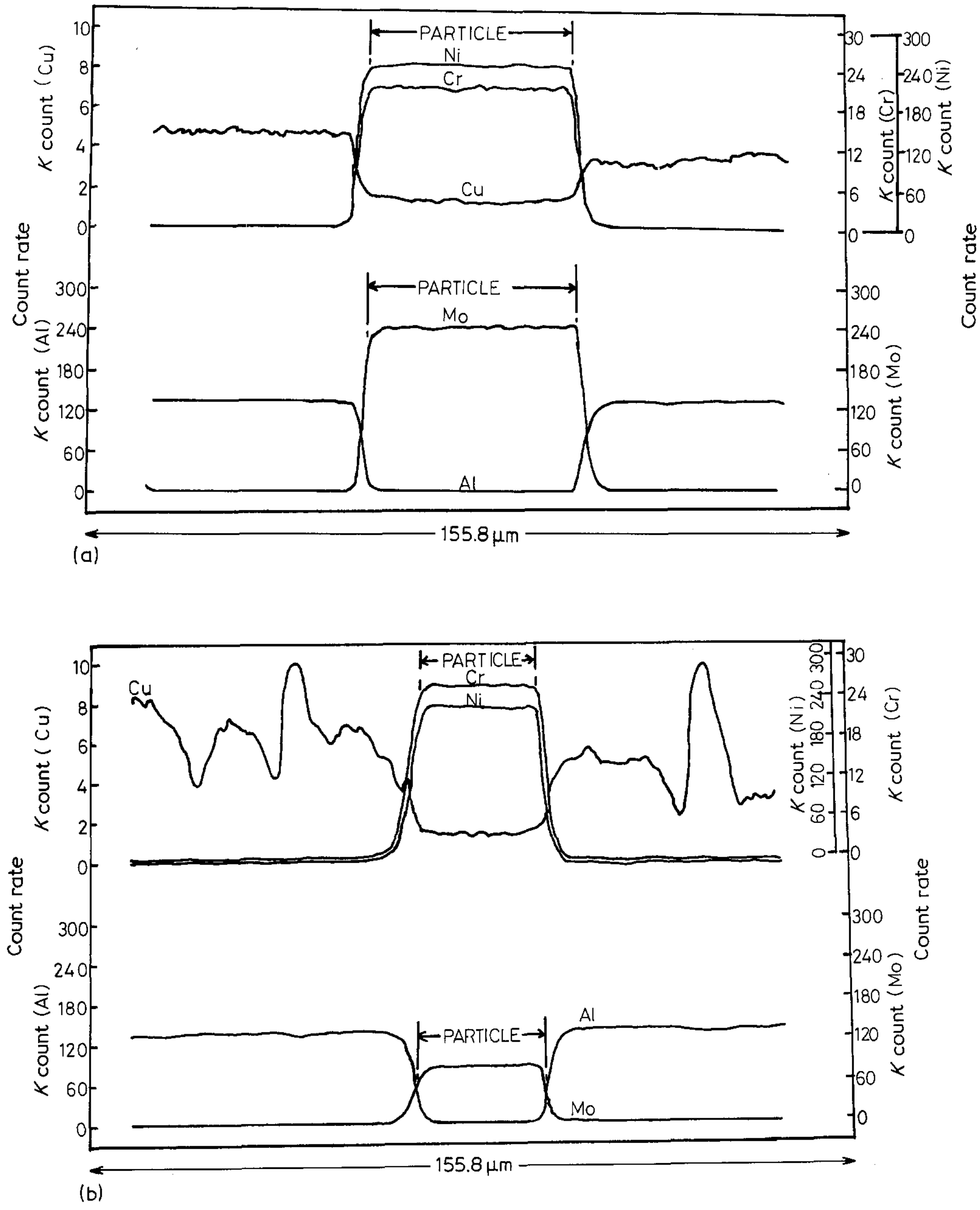

Figure 7 X-ray elemental line analysis of chromium, nickel, molybdenum, aluminium and copper across a metallic glass particle in 2014 aluminium alloy (a) sintered at 570° C and (b) sintered at 550° C. (Units of count rate: k counts sec^{-1}.)

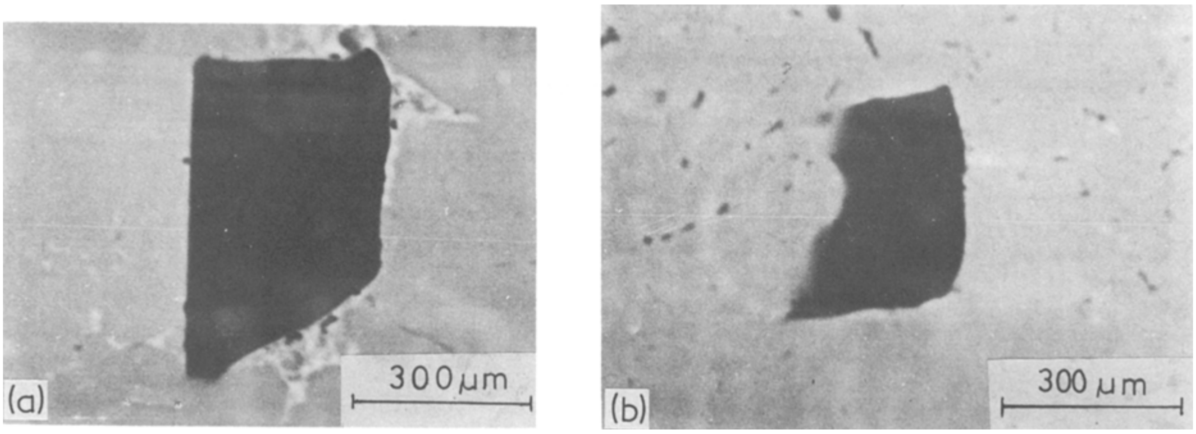

Figure 8 Photomicrographs of the particles through which a probe was run in the EPMA study: (a) composite sintered at 570° C, (b) sintered at 550° C.

hardness predicted by the rule of mixtures [17]. In fact the system should be treated as a three-phase material containing aluminium alloy matrix, metallic glass particles and porosity.

The maximum hardness after argon sintering compared to that for other atmospheres is attributed to the relatively low dew point of argon, and the lack of any volatilization of the alloying element (magnesium). Dudas and Dean [1] previously reported the above behaviour for 2014 aluminium alloy. An increase in hardness after re-pressing is a natural consequence of the reduction in pores and the work-hardening of composites.

4.3. Electrical resistivity

The resistivity value of sintered and aged 2014 aluminium alloy without any dispersoids (50 nΩ m at 16% porosity) as presently reported, is higher than the resistivity of wrought 2014 aluminium alloy (34 nΩ m) reported earlier [18]. This was due to the presence of large amounts of porosity in P/M compacts compared to the wrought product, which contains hardly any porosity. The variation in electrical resistivity with dispersoid content in the composites shows that the resistivity increased with increase in the dispersoid content. Porosity, together with the fact that the metallic glass has a higher resistivity than the aluminium alloy, would result in an increased resistivity of composites as compared to the matrix (Figs. 3 to 5). A nitrogen atmosphere, due to its relatively high dew point, could result in more oxide formation in the composites as compared to other sintering atmospheres (argon and vacuum), leading to a higher electrical resistivity for composites sintered in nitrogen. The low resistivity of re-pressed and re-sintered composites is due to the lower porosity of such composites.

4.4. Corrosion behaviour

It has been reported that amorphous metallic glass is highly resistant to corrosion [19]. With the incorporation of metallic glass in aluminium alloy matrix, one would normally expect a decrease in the corrosion rate of the composite as compared to the matrix alloy. However, the potentials between the matrix and dispersoid are also different and this might result in an increase in the corrosion rate of the composite as compared to the matrix alloy. It can be seen from Fig. 6 that the corrosion rate of composites decreased with increasing amount of dispersoid. This observation requires comprehensive investigation before possible mechanisms can be proposed. It can also be seen from Fig. 6 that re-pressed and re-sintered composites showed a further decrease in the corrosion rate. This decrease in corrosion rate could be due to the decrease in porosity in re-pressed and re-sintered composites.

5. Conclusions

1. The hardness *Hv* of power-metallurgy produced composites of 2014 aluminium alloy with metallic glass (Ni–Mo based) increased from 40 to 55 kg mm^{-2} with the dispersion of 4 vol % of metallic glass. Above this volume fraction the hardness was found to decrease, apparently due to increasing porosity. A maximum hardness of 83 kg mm^{-2} was attained by the same composite after re-sintering and re-pressing.
2. Dimensional growth of up to 6% in a linear dimension was observed for the composite containing 20 vol % of metallic glass sintered in a vacuum.
3. The electrical resistivity was found to increase with increasing amount of metallic glass particles. A maximum electrical resistivity of 180 nΩ m was observed for composites containing 12 vol % of metallic glass sintered in a nitrogen atmosphere.
4. The corrosion rate of composites in an artificial sea water environment decreased linearly with the volume fraction of metallic glass from 80×10^{-3} (for the base alloy) to 18×10^{-3} mg dm^{-2} per day (for composites containing 20 vol % of metallic glass). Re-pressing and re-sintering resulted in a further decrease of 28% in the corrosion rate.

Acknowledgements

The authors thank Dr S. V. Prasad for useful discussions, Dr J. A. Sekhar, Scientist, Defence Metallurgical Research Laboratory for EPMA data, and Mr O. P. Modi for corrosion studies.

References

1. J. N. DUDAS and W. A. DEAN, *Int. J. Powder Metall.* **5** (1969) 24.
2. J. N. DUDAS and C. B. THOMPSON, in "Modern Developments in Powder Metallurgy", Vol. 5, edited by H. H. Hausner (MPIF, Princeton, 1971) p. 19.
3. P. F. MATHEWS, *Inst. J. Powder Metall.* **4** (1968) 39.
4. J. P. LYLE, Jr, W. S. CEBULAK and K. E. BUCHOVSKY, in "Progress in Powder Metallurgy", Vol. 28, edited by A. S. Buffered (MPIF, Princeton, 1972) p. 93.
5. H. M. LEDBETTER and S. K. DATTA, *Mater. Sci. Eng.* **67** (1) (1984) 25.
6. G. JANGG, F. KUTNER and G. KORB, *Powder Metall. Int.* **1** (9) (1977) 24.
7. F. V. LENEL, G. S. ANSELL and E. C. NELSON, *Trans. AIME* **209** (1957) 117.
8. NIELS HANSEN, *Powder Metall.* **10** (20) (1967) 94.
9. S. CERESARA and P. FIORINI, *ibid.* **24** (4) (1981) 210.
10. B. A. WILCOX, AFMI–TR–72–238 (1972); cited in "Dispersion Strengthened Metal", (Metal and Ceramic Information Centre, Battelle, Columbus Laboratories, USA, 1977).
11. A. K. JHA and G. S. UPADHYAYA, *Trans. Powder Metall. Assoc. India* **15** (1) (1983) 20.
12. *Idem, J. Mater. Sci. Lett.* **2** (1983) 801.
13. G. ARTHUR, *J. Inst. Metals* **83** (1954) 329.
14. W. KEHL and H. F. FISCHMEISTER, *Powder Metall.* **3** (1980) 113.
15. C. J. SMITHELLS, (ed.), "Metal Reference Book" (Butterworths, London, 1976) p. 400.
16. T. WATANABE and K. YAMADA, Report No. 19 (Casting Research Laboratory, Waseda University, Tokyo, 1968) p. 21.
17. G. C. PAPANICOLAU and P. S. THEREARIS, *Colloid Polym. Sci.* **257** (1979) 239.
18. "ASM Metal Reference Book" (ASM, Metals Park, Ohio, 1983) p. 293.
19. Marko Materials Inc. USA, US Patent 4 116 682 (1978).

Received 6 March
and accepted 17 June 1985